



โครงการ
การเรียนการสอนเพื่อเสริมประสบการณ์

ชื่อโครงการ Interaction between Sweet Taste Receptor and Sweeteners using Molecular Dynamics Simulation

การศึกษาอันตรกิริยาระหว่างตัวรับรสหวานและสารให้ความหวานด้วยการใช้แบบจำลองพลวัตเชิงโมเลกุล

ชื่อนิสิต นางสาวอัญชัญ โอภาสมหากุล

ภาควิชา เคมี

ปีการศึกษา 2559

คณะวิทยาศาสตร์ จุฬาลงกรณ์มหาวิทยาลัย

Interaction between Sweet Taste Receptor and Sweeteners using
Molecular Dynamics Simulation

การศึกษาอันตรกิริยาระหว่างตัวรับรสหวานและสารให้ความหวานด้วยการใช้
แบบจำลองพลวัตเชิงโมเลกุล

By

Miss Aunchan Opasmahakul

Submitted in partial fulfillment of the requirements for
the Bachelor of Science Program

Department of Chemistry, Faculty of Science

Chulalongkorn University

Academic Year 2016


Project Title Interaction between Sweet Taste Receptor and Sweeteners using
Molecular Dynamics Simulation

By Miss Aunchan Opasmahakul


Accepted by the Faculty of Science, Chulalongkorn University in Partial Fulfillment of the
Requirements for the Bachelor's Degree

Project Committee


..... Chairman
(Assistant Professor Kanet Wongravee, Ph.D.)


..... Project Advisor
(Professor Supot Hannongbua, Ph.D.)


..... Project Co-Advisor
(Assistant Professor Thanyada Rungrotmongkol, Ph.D.)


..... Examiner
(Associate Professor Nongnuj Muangsin, Ph.D.)

This report has been endorsed by Head of Chemistry Department

.....
(Associate Professor Vudhichai Parasuk, Ph.D.)

Head of Chemistry Department

Date..... Month..... Year.....

Overall Quality of this Report Excellent Satisfactory Somewhat Satisfactory

Project Title Interaction between Sweet Taste Receptor and Sweeteners using
Molecular Dynamics Simulation

Student Name Miss Aunchan Opasmahakul Student ID 5633172723

Advisor Name Professor Supot Hannongbua, Ph.D.

Co-advisor Name Assistant Professor Thanyada Rungrotmongkol, Ph.D.

Department of Chemistry, Faculty of Science, Chulalongkorn University,
Academic Year 2016

Abstract

The human sweet taste receptor (hT1R2-hT1R3) is the heteromeric complex composed of T1R2 and hT1R3 in the class C G-protein-coupled receptors (GPCRs). Up to date, no crystal structure of hT1R2-hT1R3 is available, and thus homology modeling was applied here to model the hT1R2-hT1R3 complex using metabotropic glutamate receptor subtype 1 as the template. The hT1R2-hT1R3 can bind with low molecular weight sweeteners such as aspartame, neotame, sucralose, xylitol and sorbitol. In the present study, the hT1R2-hT1R3 modeled complex with xylitol or sorbitol bound were studied by molecular docking and molecular dynamics simulation. The intermolecular interactions between ligand and protein as well as binding free energies suggested that both xylitol and sorbitol preferred to bind with hT1R2 rather than hT1R3. These results could provide a more understanding of interaction between human sweet taste receptor and sweeteners (xylitol and sorbitol).

Keywords: hT1R2-hT1R3, Xylitol, Sorbitol, Molecular dynamics simulation

ชื่อโครงการ การศึกษาอันตรกิริยาระหว่างตัวรับรสหวานและสารให้ความหวานด้วยการใช้
แบบจำลองพลวัตเชิงโมเลกุล

ชื่อนิสิตในโครงการ นางสาวอัญชัญ โอภาสมหากุล เลขประจำตัว 5633172723

ชื่ออาจารย์ที่ปรึกษา ศาสตราจารย์ ดร.สุพจน์ หารหนองบัว

ชื่ออาจารย์ที่ปรึกษาร่วม ผู้ช่วยศาสตราจารย์ ดร.ธัญญดา รุ่งโรจน์มงคล

ภาควิชาเคมี คณะวิทยาศาสตร์ จุฬาลงกรณ์มหาวิทยาลัย ปีการศึกษา 2559

บทคัดย่อ

ตัวรับรสหวานในมนุษย์ (hT1R2-hT1R3) เป็นโปรตีนตัวรับแบบคู่จีตราสซี ประกอบด้วยโปรตีน hT1R2 และ hT1R3 ในปัจจุบันยังไม่มีโครงสร้างสามมิติของตัวรับรสหวานในมนุษย์ ในงานวิจัยนี้จึงทำการจำลองโครงสร้างสามมิติด้วยวิธีโฮโมโลยีโมเดลโดยใช้ตัวรับกลูตาเมตแบบเมทาโบทรอปิกชนิดย่อยที่ 1 เป็นโปรตีนแม่แบบ ตัวรับรสหวานในมนุษย์สามารถยึดจับกับสารให้ความหวานที่มีมวลโมเลกุลต่ำได้ เช่น แอสปาร์แตม นีโอแตม ซูคราโลส ซิลิทอล และซอร์บิทอลเป็นต้น ในงานวิจัยนี้มุ่งศึกษาการยึดจับของซิลิทอลและซอร์บิทอล กับตัวรับรสหวานในมนุษย์โดยใช้เทคนิคโมเลคิวลาร์ดอกกิงและการจำลองพลวัตเชิงโมเลกุล อันตรกิริยาระหว่างลิแกนด์และโปรตีนรวมถึงพลังงานการยึดจับอิสระชี้ให้เห็นว่าซิลิทอลและซอร์บิทอลซอลจับกับโปรตีน hT1R2 มากกว่า hT1R3 ผลการวิจัยนี้ทำให้เข้าใจอันตรกิริยาระหว่างตัวรับรสหวานในมนุษย์และสารให้ความหวาน (ซิลิทอลและซอร์บิทอล) มากยิ่งขึ้น

คำสำคัญ: ตัวรับรสหวานในมนุษย์, ซิลิทอล, ซอร์บิทอล, การจำลองพลวัตเชิงโมเลกุล

Acknowledgement

I am very grateful to my advisor, Professor Supot Hannongbua, PhD. and my co-advisor, Assistant Professor Thanyada Rungrotmongkol, Ph.D. who always give a helpful suggestion and advices along the project. I also thank to Wanwisa Panman (P'may) and Warin Jetsadawisut (P'nan) who always support with every information and give me practice in computational study.

Finally, I would like to thank my family who always give me and power to work with this project.



Contents

	Page
Abstract	iv
บทคัดย่อ	v
Acknowledgements	vi
Contents	vii
List of Figures	ix
List of Tables	x
Abbreviation Index	xi
Chapter 1 Introduction	1
1.1 Background and motivation of study	1
1.2 Objectives of the study	2
1.3 Benefits of the study	2
1.4 Related studies	2
1.5 A tongue of human	3
1.6 A sweet taste receptor	4
1.7 Xylitol and sorbitol	5
1.8 Homology modeling	6
1.9 Molecular docking simulation	6
1.10 Molecular dynamic simulation	7
Chapter 2 Methods	9
2.1 Materials	9
2.2 Preparation of human sweet taste receptor	10
2.3 Preparation of xylitol and sorbitol	12
2.4 Molecular docking simulation	13
2.5 System preparation	14
2.6 Molecular dynamics simulation	15
2.7 Binding free energy prediction	15
Chapter 3 Result and Discussion	16
3.1 Homology modeling of human sweet taste receptor	17
3.2 Molecular docking simulation	18
3.3 Molecular dynamics simulation	19

3.4 Key residues for ligand binding interaction	21
3.5 Hydrogen bonding interaction	23
3.6 Binding affinity prediction	24
Chapter 4 Conclusion	26
Suggestion and Future Works	26
References	27
Curriculum Vitae	29



List of Figures

Figure 1.1 The taste buds and papillae.	3
Figure 1.2 The shape of taste bud.	4
Figure 1.3 Taste receptor type 1 subtypes 2 and 3 (T1R2-T1R3).	5
Figure 1.4 Chemical structures of A) xylitol and B) sorbitol.	5
Figure 1.5 Docking between ligand and receptor.	6
Figure 2.1 Crystal structure of mGluR1 as template protein for constructing the hT1R2-hT1R3 modelled structure.	10
Figure 2.2 ORF Finder website.	11
Figure 2.3 Swiss Model website.	11
Figure 2.4 PROPKA website.	12
Figure 2.5 SMILES string in BIOVIA Draw 2016 program.	12
Figure 2.6 Calculation setup in GaussView 5.0 program.	13
Figure 2.7 Sphere object attributes of hT1R2 (left) and hT1R3 (right).	13
Figure 3.1 Sequence alignment between mGluR1 and hT1R2 (Dark green is same residues and light green is same structure residues).	16
Figure 3.2 Sequence alignment between mGluR1 and hT1R3 (Dark green is same residues and light green is same structure residues).	17
Figure 3.3 Superimposition between mGluR1 template (pink) and human sweet taste receptor (green).	17
Figure 3.4 Homology model of human sweet taste receptor.	18
Figure 3.5 hT1R2 and hT1R3 of xylitol were selected for molecular dynamics simulation of the complexes.	19
Figure 3.6 Root-mean square displacement (RMSD) of A) xylitol and B) sorbitol in complex with hT1R2-hT1R3.	20
Figure 3.7 Per-residue decomposition free energy ($\Delta G_{\text{bind}}^{\text{residue}}$) of hT1R2 (red) and hT1R3 (blue) for xylitol and sorbitol.	21
Figure 3.8 Averaged energy contributions over the MD simulations.	22
Figure 3.9 Percentage of hydrogen bonding occupation of the hT1R2-hT1R3 residues contributed to A) xylitol and B) sorbitol over the last 30-ns MD simulations.	24

List of Tables

Table 2.1 Total atoms in the two focused systems of sweeteners/hT1R2-hT1R3 complex.	14
Table 3.1 The lowest binding energy (kcal/mol) of xylitol and sorbitol at hT1R2 and hT1R3.	19
Table 3.2 The averaged binding free energy and its components (kcal/mol) of the hT1R2 and hT1R3 binding to xylitol and sorbitol.	25



Abbreviation Index



T1R2	taste receptor type 1 subtypes 2
T1R3	taste receptor type 1 subtypes 3
hT1R2-hT1R3	human sweet taste receptor
mGluR1	metabotropic glutamate receptor subtypes 1
GPCRs	G protein-coupled receptors
VFTM	Venus Flytrap Module
CRD	cysteine rich domain
TMD	7-helix transmembrane domain
MD	molecular dynamics
PDB	Protein Data Bank
RMSD	root mean square deviation
MM/PBSA	molecular mechanics/poisson-boltzmann surface area
MM/GBSA	molecular mechanics/generalized born surface area
AMBER	assisted model building with energy refinement
SD	steepest descents
CG	conjugated gradient
PME	particle mesh Ewald
PMEMD	particle mesh Ewald molecular dynamics

Chapter 1

Introduction

1.1 Background and motivation of study

Xylitol and sorbitol are known as low energy sweeteners. They have lower calories and are much sweeter than sucrose. Xylitol is categorized as a sugar alcohol like sorbitol, but xylitol has 5 carbon atoms which is 1 atom lower than sorbitol. The resemblance of structures of xylitol and sorbitol make them share something in common. They are actively beneficial for dental health by reducing caries and can be used to prepare foods for diabetes patients. Xylitol and sorbitol (also known as glucitol) are produced by catalytic hydrogenation of xylose and glucose, respectively.

Human can detect all 5 tastes: sweet, bitter, sour, salty and umami through different protein receptors. Sweet taste receptor is taste receptor type 1 subtypes 2 and 3 (T1R2, T1R3). So, sweet taste receptor of human (hT1R2-hT1R3) is a heterodimer of T1R2 and T1R3. Up to date, hT1R2-hT1R3 has no crystal structure and thus homology modeling is used to predict the 3D structure of this complex. Then, xylitol and sorbitol are separately docked into the ligand-binding sites of hT1R2-hT1R3 by using molecular docking simulation in order to get the initial structure for molecular dynamics study.

In this study, we studied the sweeteners (xylitol and sorbitol) binding to the ligand binding sites of hT1R2 and hT1R3 using molecular dynamics simulation. The binding free energies of sweetener at the binding sites of hT1R2 and hT1R3 were investigated and compared. The critical residues important in the sweetener binding were also identified. All of these results can increase our understanding about the interactions between hT1R2-hT1R3 and sweeteners.

1.2 Objectives of the study

1.2.1 To compare the efficiency of sweetener binding free energy at the ligand binding sites of hT1R2 and hT1R3.

1.2.2 To identify the critical residues important in the sweetener binding.

1.3 Benefits of the study

Increased understanding about the interactions between hT1R2-hT1R3 and sweeteners could be further helpful in sweetener design.

1.4 Related studies

In 2012, Masuda et al [1] studied about characterizing the modes of binding between hT1R2-hT1R3 and low-molecular-weight sweet compounds by functional analysis and molecular docking simulation at the binding pocket of hT1R2. They determined the amino acid residues responsible for binding to sweeteners in the cleft of hT1R2. They used mGluR1 crystal structure from Kunishima et al's [2] study for creating a homology modeling which looked same as Mailliet et al's [3]. They could deeply characterize and identify critical residues along with two water molecules between hT1R2-hT1R3 and aspartame. They showed that the binding depended on two water molecules and 11 amino acid residues in the binding pocket. All of the studies can bring the understanding of binding pocket of hT1R2 in molecule.

1.5 A tongue of human

Humans can detect and identify the 5 tastes: sweet, bitter, salty, sour, and umami by their tongue, palate, epiglottis, and upper esophageal because these organs have taste buds and the tongue is the organ that has the most taste buds among the others [4].

A Tongue can be categorized into 3 sites by papillae with the taste buds [5]. (Figure 1.1)

1. Circumvallate papillae, which can be found at the very back of a tongue.
2. Foliate papillae, which can be found at in the anterior two-thirds.
3. Fungiform papillae, which can be found at the posterior literal edge of the tongue.

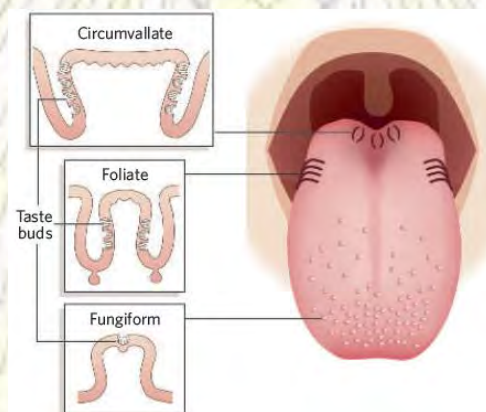


Figure 1.1 The taste buds and papillae [6].

The taste buds are composed of 50-100 taste receptor cells. Upper and lower of taste receptor cells are sharp. The top of taste buds are called taste pore and the bottom of taste buds have many nerves that help detect and transmit taste signals to the brain [5]. (Figure 1.2)

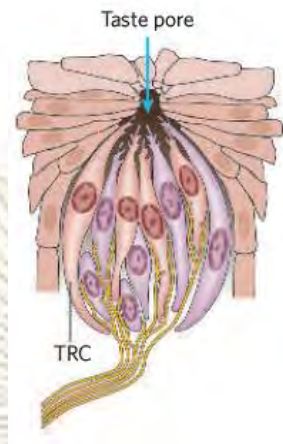


Figure 1.2 The shape of taste bud [6].

1.6 A sweet taste receptor

When we eat food, substances are digested by enzyme in saliva. The result of the digestion will cause transduction, which is a process that can convert chemical energy into electro chemical energy. Taste receptor cells in taste buds have 2 types: a receptor protein that is the protein channel called G protein-coupled taste receptors and ion channel. A taste receptor is a protein channel which facilitates the sensation of taste [7]. Taste receptor type 1; subtypes 2 and 3 (T1R2-T1R3) are heteromeric complex that detect of all sweet taste stimuli. T1R2-T1R3 are in class C G protein-coupled receptors (GPCRs) and related to metabotropic glutamate receptor (mGluRs) [8]. T1R2-T1R3 are a large extracellular terminal domain composed of Venus Flytrap Module (VFTM), cysteine rich domain (CRD), and 7-helix transmembrane domain (TMD) [9]. (Figure 1.3)

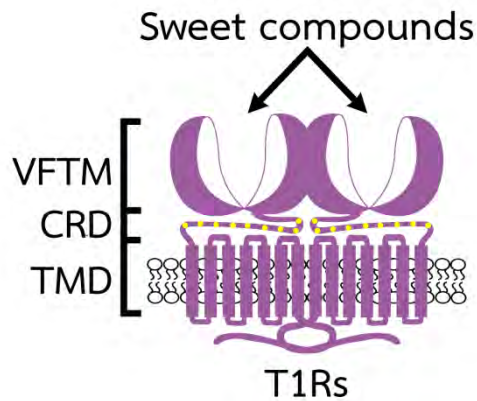


Figure 1.3 Taste receptor type 1 subtypes 2 and 3 (T1R2-T1R3).

1.7 Xylitol and sorbitol

Xylitol and sorbitol are sugar alcohol used as sweeteners. Xylitol is found in many fruits and vegetables for example birch, cabbage, and strawberry. Sorbitol is found in many fruits for example corn, cassava, and potato. Xylitol and sorbitol are sweeter than sucrose, and have lower calories. Xylitol has 5 carbon atoms that are lower than sorbitol 1 atom (Figure 1.4). Xylitol is produced by catalytic hydrogenation of xylose. Sorbitol is produced by catalytic hydrogenation of glucose. Xylitol and sorbitol are normally found as ingredients in ‘sugar-free’ candies and chewing gum. They can also be used to prevent dental caries because microorganisms cannot consume these sweeteners to survive [10].

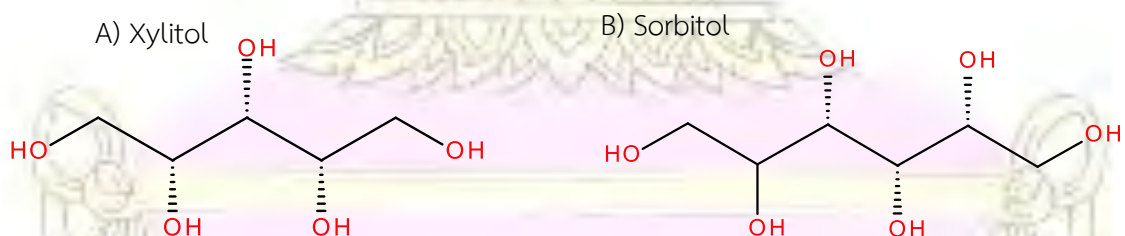


Figure 1.4 Chemical structures of A) xylitol and B) sorbitol.

1.8 Homology modeling

In the world, there is only little numbers of protein structures with solved by experiment from many protein sequences. The computational tools are needed to solve the protein structures. The best method is homology modeling or comparative modeling [11]. This method is used to successfully predict a 3D tertiary structure of unknown protein structure using known protein templates. The protein template is crystal structure that crystallizes by X-ray crystallography experimentally, has similar protein structure with the unknown protein, and related to unknown protein evolutionarily [12]. The sequence identity between the template protein and the target sequence is more than 20 % that is agreeable [13].

1.9 Molecular docking simulation

Molecular docking simulation is the computational method which predicts the binding-conformation of small molecule ligands and a receptor at the appropriate target binding site. Molecular docking may be defined as “lock-and-key”, which one ligand wants to find the correct relative orientation of the receptor key (Figure 1.5) [14].

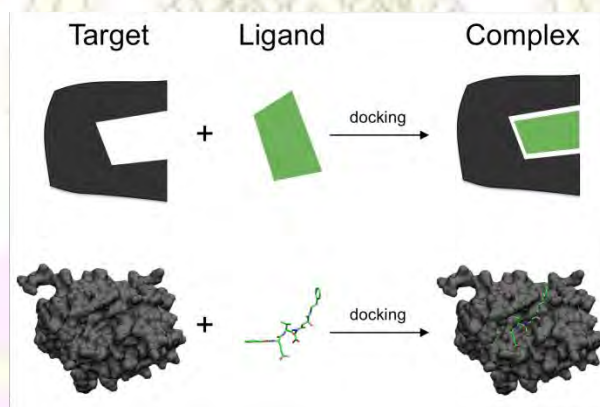


Figure 1.5 Docking between ligand and receptor.

The conformations of protein-ligand complex will be calculated using CDOCK program [15]. The various contributions to binding can be written as an additive equation [16]:

$$\Delta G_{\text{bind}} = \Delta G_{\text{solvent}} + \Delta G_{\text{conf}} + \Delta G_{\text{int}} + \Delta G_{\text{rot}} + \Delta G_{\text{t/t}} + \Delta G_{\text{vib}}$$

where ΔG_{bind} is energy of the pose within the binding site.

$\Delta G_{\text{solvent}}$ is components consist of solvent effects.

ΔG_{conf} is conformational changes in the protein and ligand.

ΔG_{int} is free energy due to protein-ligand interactions.

ΔG_{rot} is internal rotations.

$\Delta G_{\text{t/t}}$ is energy of ligand and receptor to form a single complex.

ΔG_{vib} is free energy due to changes in vibrational modes.

The best of protein-ligand complex has the lowest binding interaction energy. It used to the first complex for molecular dynamic simulation.

1.10 Molecular dynamics simulation

Molecular dynamics (MD) simulation is a computer method for studying the physical movements of atoms and molecules in liquids. In the most widely, Newton's equations of motion for a system of interacting particles determine the trajectories of atoms and molecules [17].

$$F_i = m_i \frac{d^2 r_i(t)}{dt^2}$$

where F_i is the force acting upon i^{th} particle at time t .

m_i is the mass of the particle.

$r_i(t) = (x_i(t), y_i(t), z_i(t))$ is the position vector of i^{th} particle.

Their potential energies are calculated using molecular mechanics force fields. The molecular systems are minimized and prepared parameters for long MD simulations using AMBER 14 package program [18].

Thermodynamic properties of the system are canonical ensemble (NVT), isothermal–isobaric (NPT) ensemble, and generalized ensembles that used to control the system. When the system is stable, its can bring data calculation for analysis.



Chapter 2

Methods

2.1 Materials

2.1.1 High-performance computing

2.1.2 Ubuntu operating system version 14.04

2.1.3 Programs and websites

2.1.3.1 Protein Data Bank (PDB)

2.1.3.2 ORF Finder

2.1.3.3 Swiss Model

2.1.3.4 PROPKA

2.1.3.5 BIOVIA Draw 2016

2.1.3.6 GaussView 5.0

2.1.3.7 Discovery Studio 3.0

2.1.3.8 CDOCKER

2.1.3.9 SSH Secure Shell

2.1.3.10 AMBER 14

2.1.3.11 EditPlus

2.1.3.12 OriginPro 8

2.1.3.13 PyMOL

2.1.3.14 VMD 1.9.2

2.1.3.15 VideoMach

2.1.3.16 Chimera 1.11.2

2.2 Preparation of human sweet taste receptor

The 3D structure of human sweet taste receptor (hT1R2-hT1R3) was built using the crystal structure of mGluR1 solved in active (glutamate-bound) form and obtained from protein data bank codes 1EWK [2] as the template protein (Figure 2.1) by homology modeling [12]. The nucleotide sequences of hT1R2 and hT1R3 were obtained from GenBank codes BK000151 and BK000152 [8], using ORF Finder website (Figure 2.2). Homology model of hT1R2-hT1R3 has been constructed with the Swiss Model website (Figure 2.3). The protonation state of all ionization residues of hT1R2-hT1R3 was characterized by PROPKA website (Figure 2.4).



1EWK
CRYSTAL STRUCTURE OF METABOTROPIC GLUTAMATE RECEPTOR SUBTYPE 1 COMPLEXED WITH GLUTAMATE

DOI: 10.2210/pdb1ewk/pdb

Classification: [SIGNALING PROTEIN](#)

Deposited: 2000-04-26 **Released:** 2000-12-18

Deposition author(s): [Kunishima, N.](#), [Shimada, Y.](#), [Jingami, H.](#), [Morikawa, K.](#)

Organism: [Rattus norvegicus](#)

Expression System: Spodoptera frugiperda

Structural Biology Knowledgebase: 1EWK (12 models >16 annotations) [SASKB.org](#)

Experimental Data Snapshot

Method: X-RAY DIFFRACTION

Resolution: 2.2 Å

wwPDB Validation

Metric	Percentile Ranks	Value
Rfree		0.229

Figure 2.1 Crystal structure of mGluR1 as template protein for constructing the hT1R2-hT1R3 modeled structure.

Open Reading Frame Finder

ORF finder searches for open reading frames (ORFs) in the DNA sequence you enter. The program returns the range of each ORF, along with its protein translation. Use ORF finder to search newly sequenced DNA for potential protein encoding segments, verify predicted protein using newly developed SMART BLAST or regular BLASTP.

This web version of the ORF finder is limited to the subrange of the query sequence up to 50 kb long. Stand-alone version, which doesn't have query sequence length limitation, is available for [Linux x64](#).

Examples (click to set values, then click Submit button):

- NC_011604 Salmonella enterica plasmid pWES-1; genetic code: 11; 'ATG' and alternative initiation codons; minimal ORF length: 300 nt
- NM_000059; genetic code: 1; start codon: 'ATG only'; minimal ORF length: 150 nt



Enter Query Sequence

Enter accession number, gi, or nucleotide sequence in FASTA format:

From: To:

Figure 2.2 ORF Finder website.

SWISS-MODEL Modelling Repository Documentation Log in Create Account

Start a New Modelling Project

Target Sequence:

(Format must be Fasta, Clustal, Promod, plain string, or a valid UniProtKB AC)

Template File:

Project Title:

Email:

By using the SWISS-MODEL server, you agree to comply with the following [terms of use](#) and to cite the corresponding [articles](#).

Supported Inputs

Sequence ▾

Uniprot AC ▾

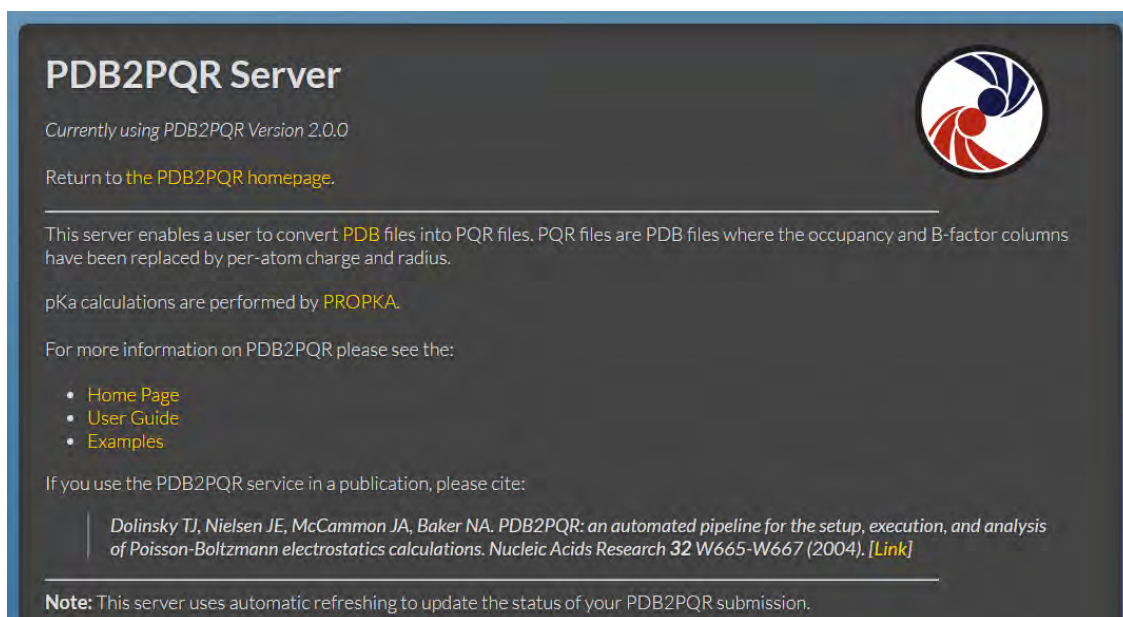
Target-Template Alignment ▾

User Template ▾

Deepview Project ▾

Hetero Project **BETA** ▾

Figure 2.3 Swiss Model website.



PDB2PQR Server

Currently using PDB2PQR Version 2.0.0

Return to [the PDB2PQR homepage](#).

This server enables a user to convert **PDB** files into PQR files. PQR files are PDB files where the occupancy and B-factor columns have been replaced by per-atom charge and radius.

pKa calculations are performed by **PROPKA**.

For more information on PDB2PQR please see the:

- [Home Page](#)
- [User Guide](#)
- [Examples](#)

If you use the PDB2PQR service in a publication, please cite:

Dolinsky TJ, Nielsen JE, McCammon JA, Baker NA. PDB2PQR: an automated pipeline for the setup, execution, and analysis of Poisson-Boltzmann electrostatics calculations. *Nucleic Acids Research* **32** W665-W667 (2004). [[Link](#)]

Note: This server uses automatic refreshing to update the status of your PDB2PQR submission.

Figure 2.4 PROPKA website.

2.3 Preparation of xylitol and sorbitol

The 3D structures of xylitol and sorbitol were built from SMILES string using BIOVIA Draw 2016 program (Figure 2.5) and then optimized by quantum calculation at the HF/6-31G* level of theory using GaussView 5.0 program (Figure 2.6).

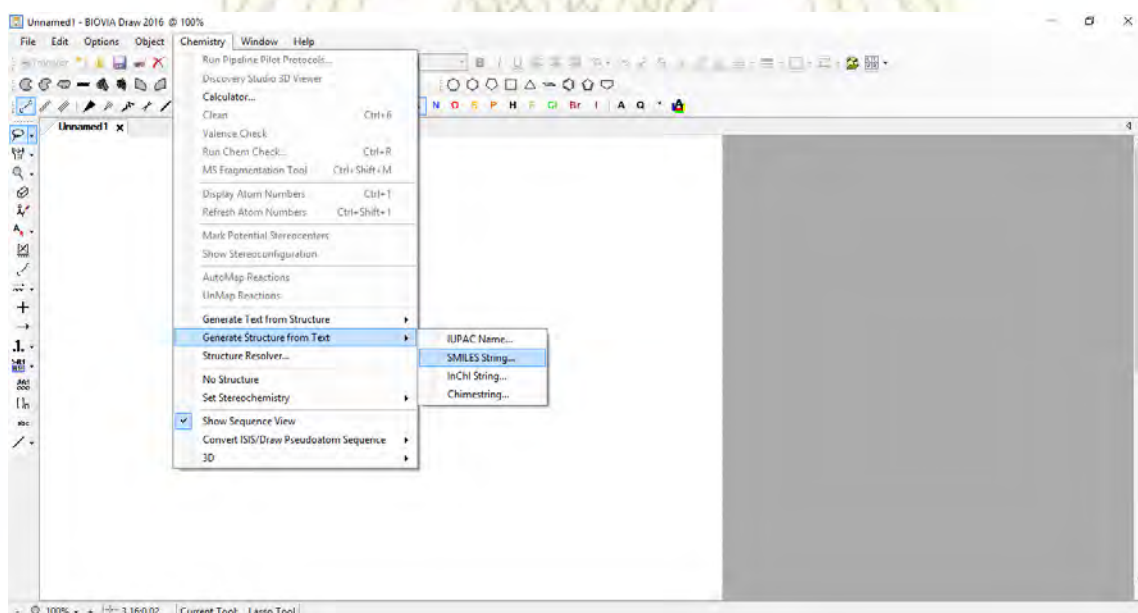


Figure 2.5 SMILES string in BIOVIA Draw 2016 program.

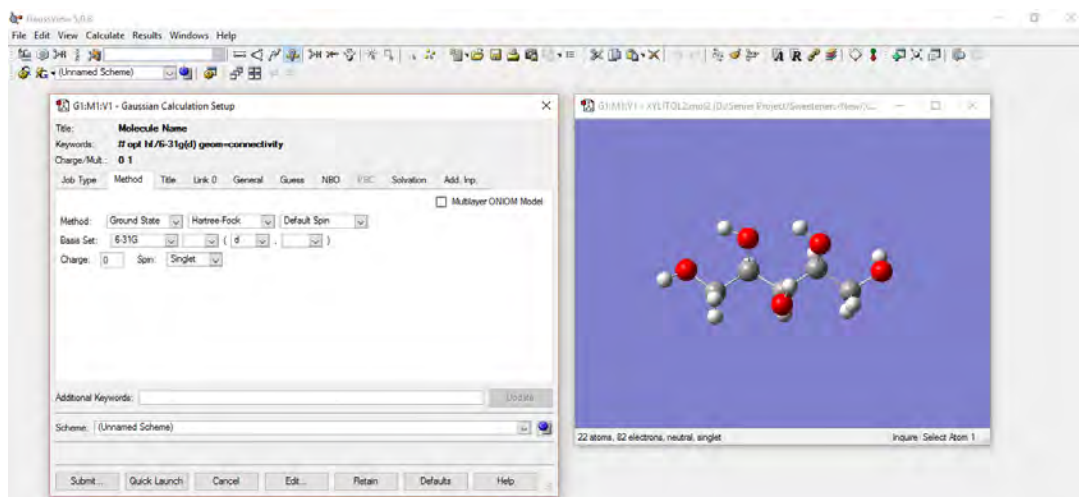


Figure 2.6 Calculation setup in GaussView 5.0 program.

2.4 Molecular docking simulation

Protein-ligand docking program, CDOCKER [15], in Discovery Studio 3.0 was used for the docking study. Xylitol and sorbitol were separately docked into the ligand-binding sites of hT1R2 and hT1R3 where glutamate is bound in the mGluR1. Docking sphere with radius of 10 Å was used (Figure 2.7). 100 poses of docking simulation were performed for each ligand. The docked complex with the lowest interaction energy was chosen as starting structure for molecular dynamics simulation.

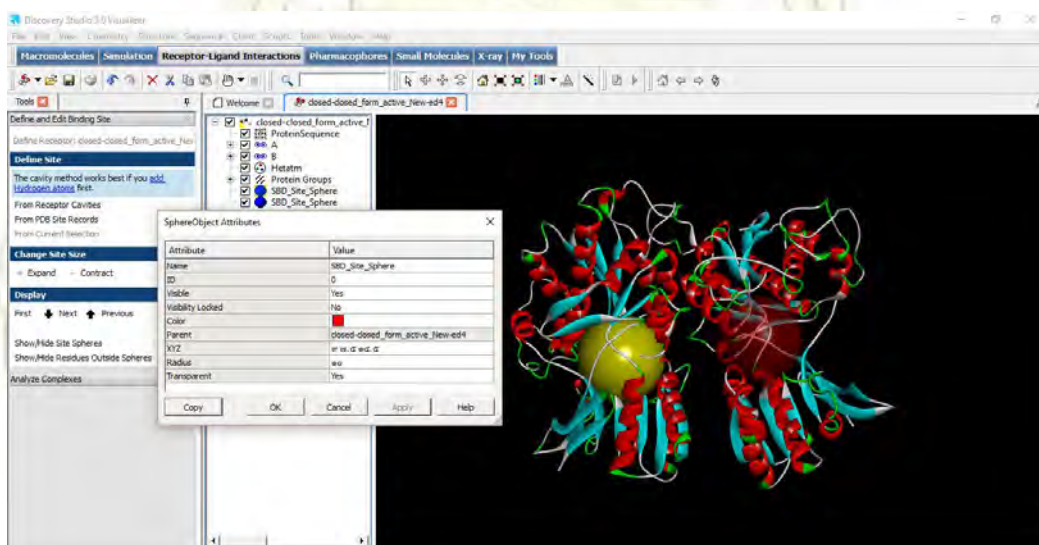


Figure 2.7 Sphere object attributes of hT1R2 (left) and hT1R3 (right).

2.5 System preparation

All system preparations were performed by AMBER14 program [18]. The missing hydrogen atoms were added using the tLEaP module in AMBER [19]. The AMBER ff12SB and gaff force field were applied for protein and ligand, respectively. Finally, each complex was solvated in the $122.78 \times 107.39 \times 119.73 \text{ \AA}^3$ rectangular box of TIP3P water model. Prior to perform MD simulation, the hydrogen atoms and water molecules were minimized with 3,000 steps of steepest descents (SD) and conjugated gradient (CG), while all protein and ligand atoms were restrained. After that, each system was minimized with restrained ligand, Na^+ , and the surrounding residues within 12 \AA from ligand. The total atoms of each system are shown in Table 2.1

Table 2.1 Total atoms in the two focused systems of sweeteners/hT1R2-hT1R3 complex.

	Total atoms	
	Xylitol	Sorbitol
hT1R2	7,243	7,243
hT1R3	7,018	7,018
Ligand	44	52
Sodium ion	20	20
Water	119,886	119,889

2.6 Molecular dynamics simulation

MD simulation was performed under periodic boundary condition. All covalent bonds involving hydrogen atom were fixed by SHAKE algorithm. The short-range cutoff of 10 Å was employed for non-bonded interactions, while the Particle Mesh Ewald (PME) summation method was applied for calculating the long-range electrostatic interactions. Langevin algorithm has been applied to control temperature with a collision frequency of 0.002 ps for the 1 ns. The system was heated up from 100.0 to 310.0 K for 0.002 ps. Afterwards, the simulation was implemented with NPT ensemble at this temperature and pressure of 1 atm using the PMEMD module in AMBER14. Each system was simulated until the simulation time reached 100 ns and the snapshots were collected 10 in every 1 ns along the simulation.

2.7 Binding free energy prediction

The binding free energy of the complex was calculated by using both MM/PBSA and MM/GBSA approaches over the 100 trajectories taken from the last 30 ns by MM/PBSA.py program in AMBER14. Moreover, the energy composition was calculated to support the binding affinity by using MM/PBSA approach and also the ligand/protein interactions in term of hydrogen bonding was measured.

Chapter 3

Result and Discussion

3.1 Homology modeling of human sweet taste receptor

By SWISS-MODEL (Figures 3.1-3.2), hT1R2 and hT1R3 have sequence identity (and similarity) with its template, mGluR1, of 24% (41%) and 22% (40%), respectively. The superimposition between mGluR1 template and the modeled structure of human sweet taste receptor using Discovery Studio 3.0 was shown in Figure 3.3, where the structure of human sweet taste receptor alone was given in Figure 3.4.



Figure 3.1 Sequence alignment between mGluR1 and hT1R2 (Dark green is same residues and light green is same structure residues).



Figure 3.2 Sequence alignment between mGluR1 and hT1R3 (Dark green is same residues and light green is same structure residues).

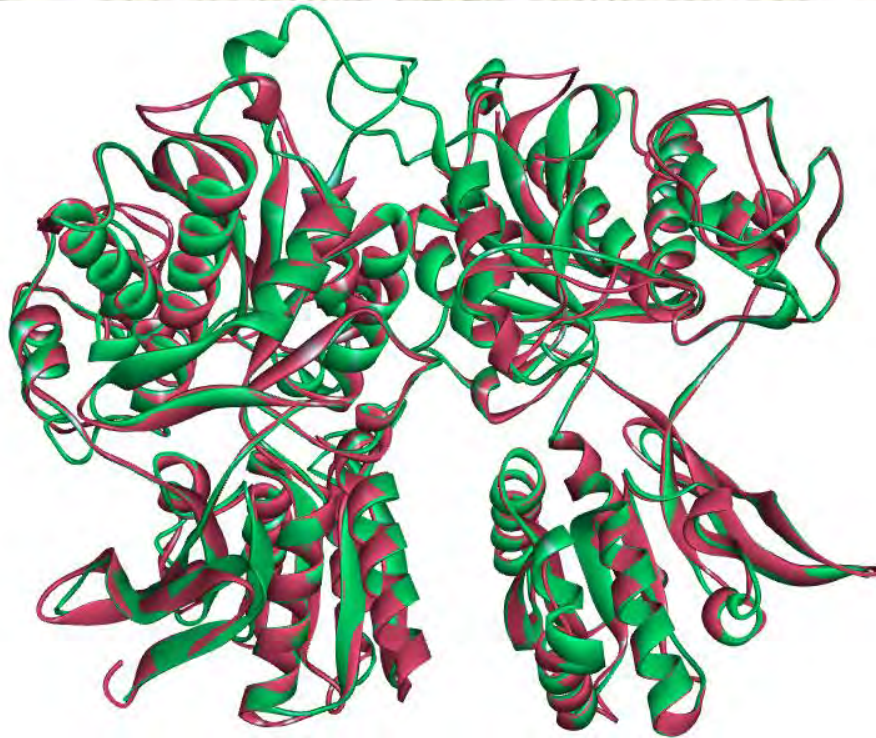


Figure 3.3 Superimposition between mGluR1 template (pink) and human sweet taste receptor (green).

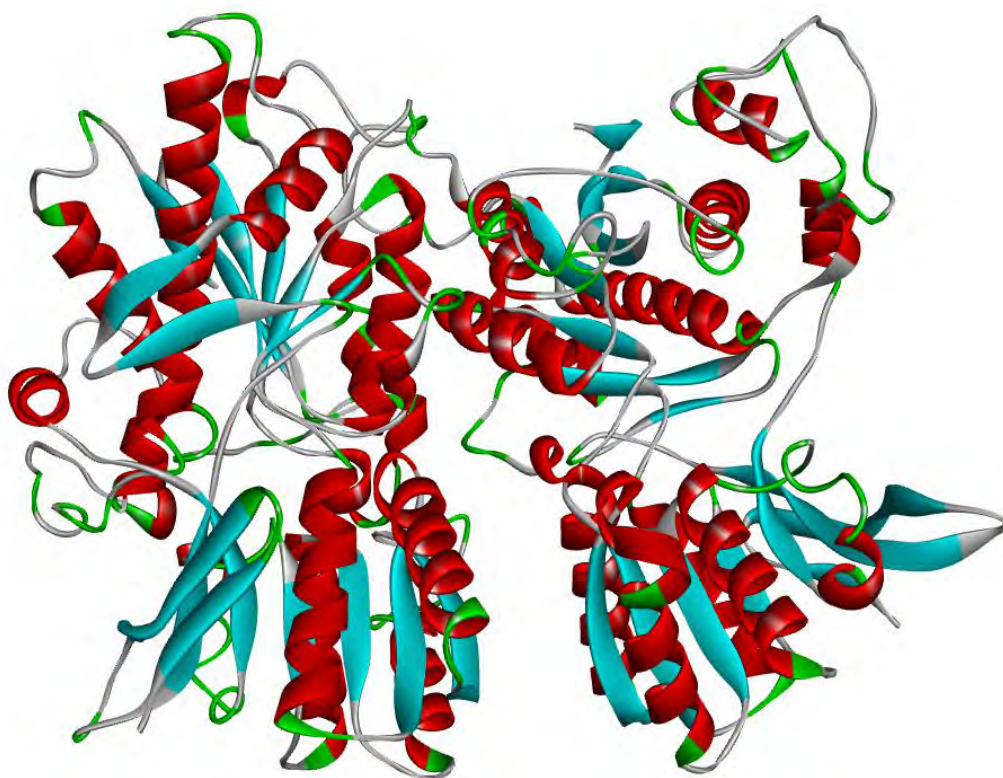


Figure 3.4 Homology model of human sweet taste receptor.

3.2 Molecular docking simulation

The geometries of xylitol and sorbitol were optimized by the HF/6-31G^{*} level of theory. CDOCKER program was used for the docking studies. Xylitol and sorbitol were docked into the binding pockets of hT1R2 and hT1R3. The configurations with lowest binding energy for xylitol at hT1R2 and hT1R3 are -34.59 kcal/mol and -26.41 kcal/mol. The configurations with lowest binding energy for sorbitol at hT1R2 and hT1R3 are -40.44 kcal/mol and -29.48 kcal/mol (Table 3.1). So, it shows that hT1R2 of xylitol and sorbitol were selected for molecular dynamics simulation of the complexes (Figure 3.5).

Table 3.1 The lowest binding energy (kcal/mol) of xylitol and sorbitol at hT1R2 and hT1R3.

	hT1R2	hT1R3
xylitol	-34.59	-26.41
sorbitol	-40.44	-29.48

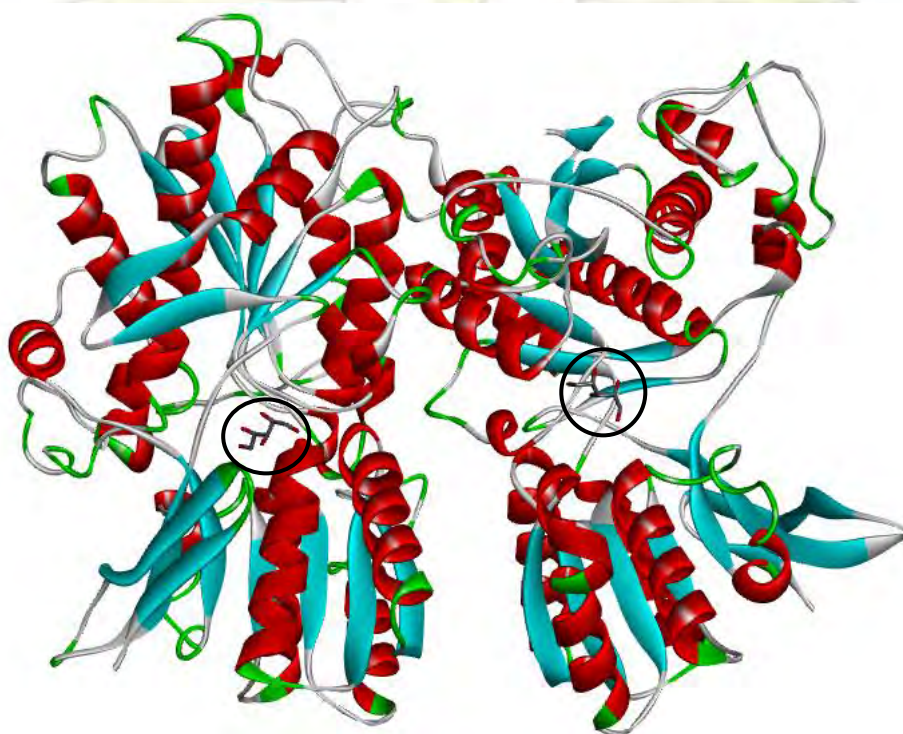


Figure 3.5 hT1R2 and hT1R3 of xylitol were selected for molecular dynamics simulation of the complexes.

3.3 Molecular dynamics simulation

A 100-ns MD simulation of xylitol and sorbitol binding to hT1R2 and hT1R3, has been performed at 310.0 K. The root-mean square displacement (RMSD) of each system was calculated to estimate the system stability along the simulation time compared to the minimized structure as plotted in Figure 3.6.

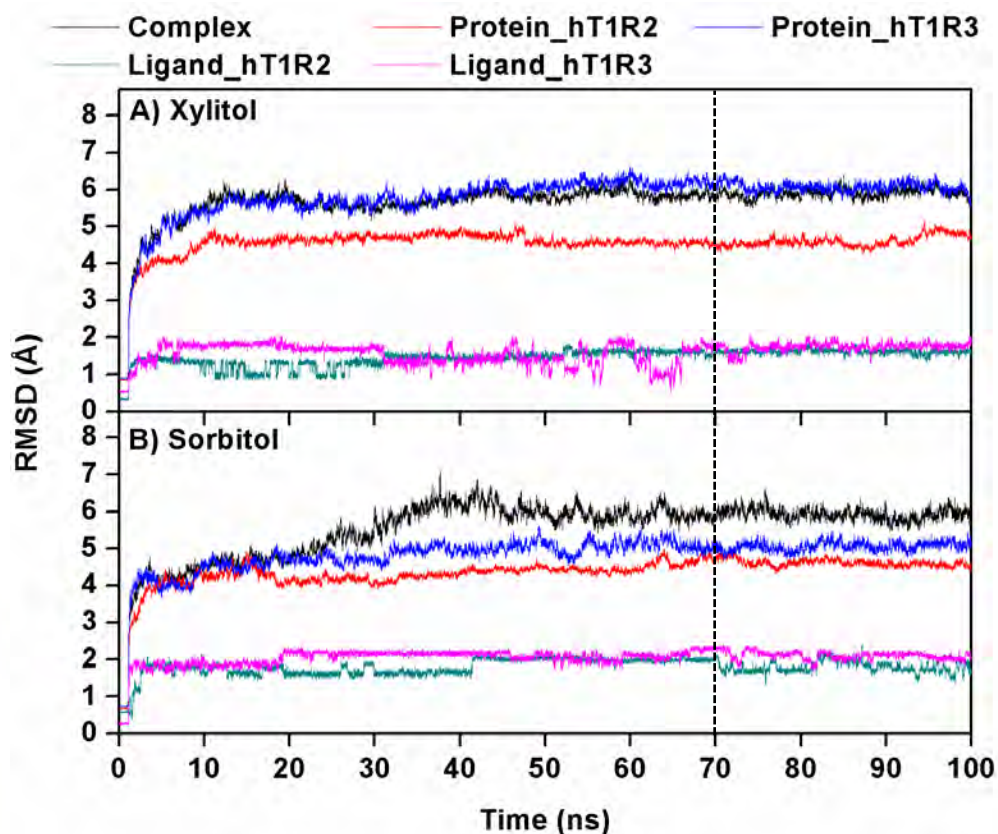


Figure 3.6 Root-mean square displacement (RMSD) of A) xylitol and B) sorbitol in complex with hT1R2-hT1R3.

The RMSD values of complex and each protein rapidly increased then fluctuated around 4-6 Å along the simulation. Until 15 ns and 40 ns for xylitol and sorbitol, the RMSD values of complex and the two proteins fluctuated from 4 to 6 Å. Xylitol and sorbitol showed RMSD values fluctuated around 1.5 Å and 2.0 Å along the simulation. The two MD systems likely tended to be stable in range of 70-100 ns. Hence, the MD trajectories from this range were taken for further analysis in terms of hydrogen bonding interaction, the decomposition energy and the binding free energy.

3.4 Key residues for ligand binding interaction

Based on MM/PBSA method, the per-residue decomposition energy ($\Delta G_{\text{bind}}^{\text{residue}}$) and its energetic components (electrostatic ($\Delta E_{\text{ele}} + \Delta G_{\text{polar}}$) and van der Waals ($\Delta E_{\text{vdW}} + \Delta G_{\text{non-polar}}$) terms) have been estimated and compared between xylitol and sorbitol binding at the hT1R2 and hT1R3 pocket. The key binding residues for xylitol and sorbitol are shown in Figures 3.7 and 3.8. The positive and negative values of per-residue decomposition free energy specify the ligand destabilization and stabilization, respectively, so the result can specify the key residue of hT1R2-hT1R3 for ligand binding interaction.

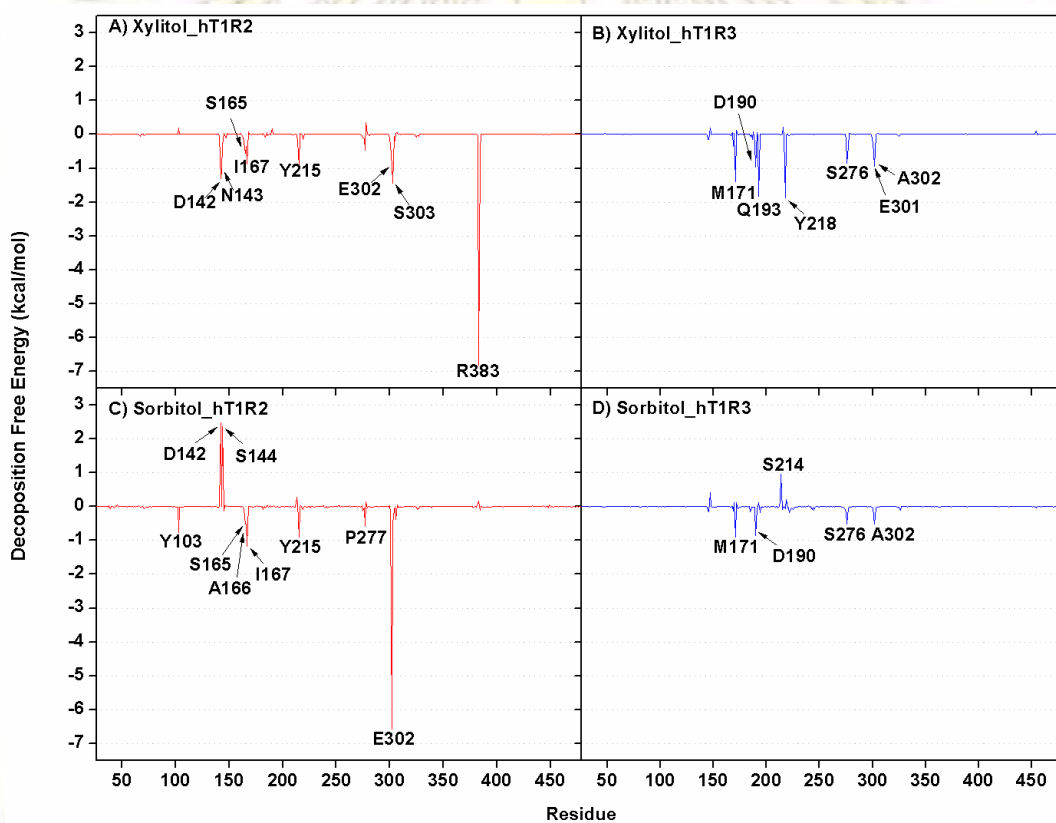


Figure 3.7 Per-residue decomposition free energy ($\Delta G_{\text{bind}}^{\text{residue}}$) of hT1R2 (red) and hT1R3 (blue) for xylitol and sorbitol.

As shown in Figure 3.7, xylitol and sorbitol have strong binding with the hT1R2 residue, R383 (-7.0 kcal/mol) and E302 (-6.5 kcal/mol), respectively. In Figure 3.7 A-B, the hT1R2 amino acids (D142, N143, S165, I167, Y215, E302, S303 and R383) and the hT1R3 amino acids (M171, D190, Q193, Y218, S276, E301 and A302) are the key residues that stabilize the binding by providing the energy contribution over -0.5 kcal/mol. Similarly in Figure 3.7 C-D, the hT1R2 amino acids (Y103, S165, A166, I167, Y215, P277 and E302) and the hT1R3 amino acids (M171, D190, S276, and A302) are the key residues that stabilize the binding by contributing over -0.5 kcal/mol. The results likely indicate that both sweeteners have good binding in the hT1R2 pocket.

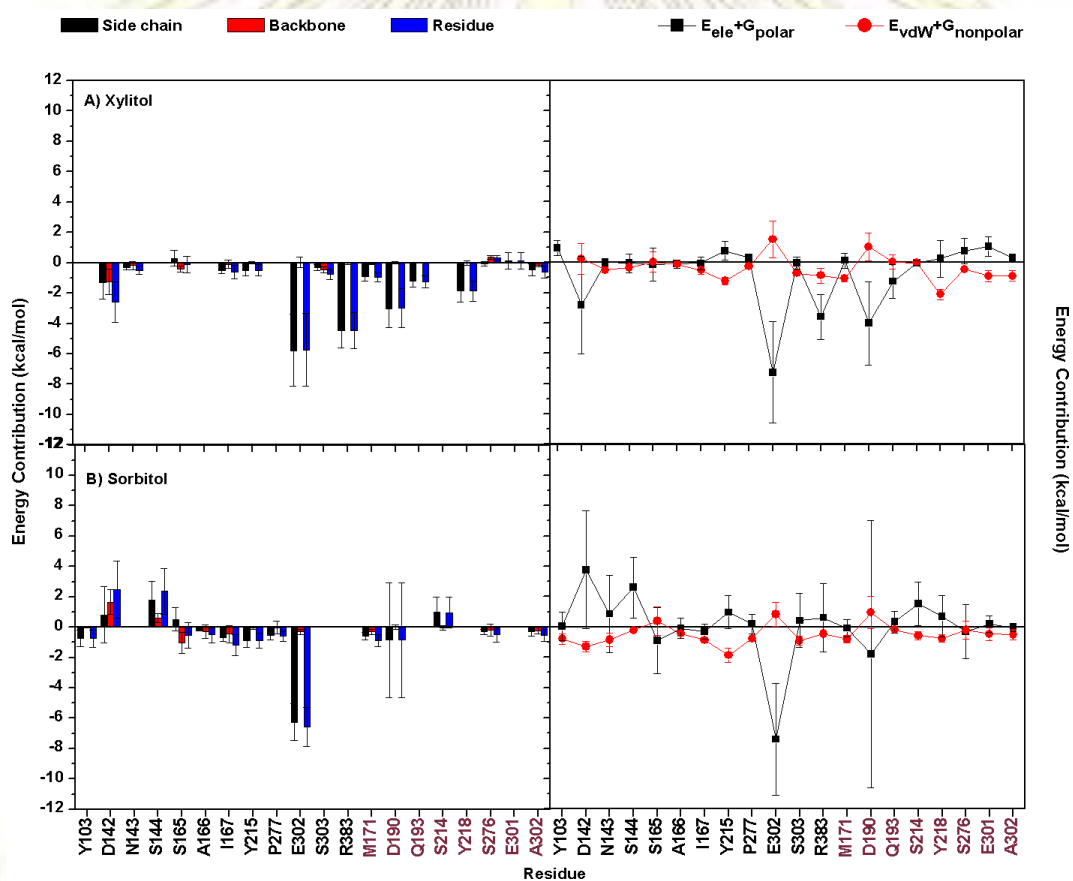


Figure 3.8 (Left) Averaged energy contributions over the MD simulations from the residue backbone and side chain for the two studied complexes of the hT1R2-hT1R3 with A) xylitol, and B) sorbitol. (Right) Averaged electrostatic ($\Delta E_{\text{ele}}^* + \Delta G_{\text{polar}}^*$) and vdW ($\Delta E_{\text{vdW}}^* + \Delta G_{\text{non-polar}}^*$) energy contributions from each residue. Note the standard deviation among the MD simulations is shown as an error bar.

Among the 12 hT1R2 residues and the 8 hT1R3 residues plotted in Figure 3.8 (left), most residues likely stabilized the ligand through their side chain such as residues Y103, S144, I167, M171, D190, Q193, S214, Y215, Y218, P277, and E302. From Figure 3.8 (right), it can be seen that electrostatic interaction plays an important role in hT1R2-hT1R3 binding with xylitol and sorbitol energy contribution up to -8 kcal/mol, while the van der Waals (vdW) interaction causes energy contribution up to -3 kcal/mol. Most residues likely stabilized the ligand through the side chain. Comparison between xylitol and sorbitol, hT1R2 D142 can only stabilize xylitol mainly via electrostatic interaction. The residue E302 in hT1R2 and the residue D190 in hT1R3 have similar contribution in term of the electrostatic interaction towards the ligand binding. Taken altogether, the electrostatic interaction plays an important role in hT1R2-hT1R3 binding with xylitol and sorbitol.

3.5 Hydrogen bonding interaction

Intermolecular hydrogen bonding interaction is essential for stabilizing ligand binding. In this work, hydrogen bonding was defined as the distance between donor and acceptor atoms below 3.5 Å and the angle between donor, hydrogen and acceptor atoms over 120 degree. From Figure 3.8, in comparison between two ligands, hydrogen bond formation with hT1R2-hT1R3 was higher detected with xylitol. More hydrogen bonding interactions of both sweeteners were found in hT1R2 in a good agreement with the decomposition energy results in Figure 3.7. Xylitol and sorbitol were formed strong hydrogen bonding with the hT1R2 E302 and the hT1R3 D190. Furthermore, the residues S165 and Y215 in hT1R2 as well as the residues D190 and D193 were also able to interact with the -OH group of xylitol and sorbitol as illustrated in Figure 3.9.

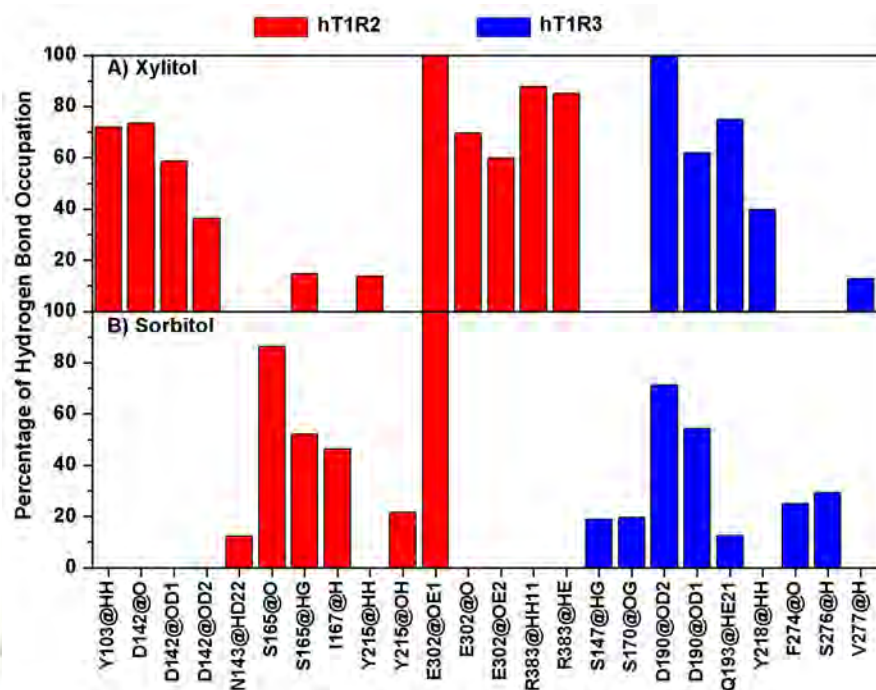


Figure 3.9 Percentage of hydrogen bonding occupation of the hT1R2-hT1R3 residues contributed to A) xylitol and B) sorbitol over the last 30-ns MD simulations.

3.6 Binding affinity prediction

To investigate the binding affinity of the focused sweetener at the two binding sites of hT1R2-hT1R3 in this study, the MM/PBSA and MM/GBSA methods were employed. The results are given in Table 3.1 together with its energetic components, the gas phase energy (ΔE_{MM}) as a summation of ΔE_{vdW} and ΔE_{ele} energies, and the solvation free energy (ΔG_{sol}). The ΔE_{ele} contribution is stronger than ΔE_{vdW} in both simulations. By including the solvation free energy, the vdW term ($\Delta G_{nonpolar,sol} + \Delta E_{vdW}$) was favorable to the total binding free energies of the two complexes, which was opposed by the unfavorable electrostatic term ($\Delta G_{ele,sol} + \Delta E_{ele}$). From both methods, it can be clearly seen that averaged binding affinity of hT1R2 with xylitol was significantly better than hT1R3 as same as sorbitol indicating the preferable binding of such sweeteners in hT1R2 rather than hT1R3. Moreover, the xylitol binding with hT1R2 was stronger than that of sorbitol as supported by the results mentioned earlier.

Table 3.2 The averaged binding free energy and its components (kcal/mol) of the hT1R2 and hT1R3 binding to xylitol and sorbitol.

	Xylitol/hT1R2	Xylitol/hT1R3	Sorbito/hT1R2	Sorbito/hT1R3
PBSA				
ΔE_{ele}	-97.24±8.72	-37.35±4.40	-60.61±8.32	-41.22±12.96
ΔE_{vdW}	-11.53±3.35	-15.17±2.26	-20.00±1.91	-16.33±2.42
ΔE_{MM}	-108.77±7.36	-52.52±4.42	-80.61±7.92	-57.55±12.50
$\Delta G_{\text{nonpolar,sol}}$	-3.05±0.07	-2.72±0.14	-3.55±0.07	-3.52±0.11
$\Delta G_{\text{ele,sol}}$	88.65±5.57	45.54±4.71	78.43±7.37	60.64±6.14
ΔG_{sol}	85.60±5.59	42.83±4.62	74.88±7.38	57.13±6.20
$\Delta G_{\text{ele,sol}} + \Delta E_{\text{ele}}$	-8.59±10.35	-8.19±6.44	17.82±11.11	19.42±14.34
$\Delta G_{\text{nonpolar,sol}} + \Delta E_{\text{vdW}}$	-14.58±3.35	-17.89±2.26	-23.55±1.91	-19.85±2.42
ΔG_{total}	-23.18±4.11	-9.70±2.92	-5.73±3.80	-0.42±7.44
$-T\Delta S$	4.47±2.64	5.20±1.77	4.49±1.40	3.79±1.34
$\Delta G_{\text{bind(MM/PBSA)}}$	-27.65±4.88	-14.90±3.41	-10.22±4.05	-4.21±7.56
GBSA				
ΔE_{ele}	-97.24±8.72	-37.35±4.40	-60.61±8.32	-41.22±12.96
ΔE_{vdW}	-11.53±3.35	-15.17±2.26	-20.00±1.91	-16.33±2.42
ΔE_{MM}	-108.77±7.36	-52.52±4.41	-80.61±7.92	-57.55±12.50
$\Delta G_{\text{nonpolar,sol}}$	-3.76±0.08	-2.78±0.09	-4.22±0.15	-3.37±0.22
$\Delta G_{\text{ele,sol}}$	91.92±6.53	50.35±3.09	73.13±6.45	58.86±12.32
ΔG_{sol}	88.16±6.49	47.56±3.06	68.91±6.38	55.49±12.25
$\Delta G_{\text{ele,sol}} + \Delta E_{\text{ele}}$	-5.32±10.94	13.00±5.38	12.52±10.53	17.64±17.88
$\Delta G_{\text{nonpolar,sol}} + \Delta E_{\text{vdW}}$	-15.29±3.35	-17.95±2.26	-24.22±1.91	-19.70±2.42
ΔG_{total}	-20.61±3.46	-4.96±2.78	-11.70±3.03	-2.06±2.44
$-T\Delta S$	4.47±2.64	5.20±1.77	4.49±1.40	3.79±1.34
$\Delta G_{\text{bind(MM/GBSA)}}$	-27.65±4.88	-14.90±3.41	-10.22±4.05	-4.21±7.56

Chapter 4

Conclusion

The hT1R2-hT1R3 systems with sweeteners bound have reached equilibrium at 70 ns and thus the trajectories taken from the last 30 ns were used for analysis. Intermolecular interaction, per-residue decomposition energy data and the total MM/PBSA and MM/GBSA binding free energies evidently showed that xylitol and sorbitol have a good binding affinity towards hT1R2 more than hT1R3.

Suggestion and Future Works

The most problem tissue in this project is the timing on high-performance computer that is always got damage to affect the system and its falls down. It causes a delay to finish work and need too much time for download and backup all data. So, the newly high performance computer is required to work safe with every research.

References

- [1] Masuda, K.; Koizumi, A.; Nakajima, K.; Tanaka, T.; Ade, K.; Misaka, T.; Ishiguro, M. Characterization of the Modes of Binding between Human Sweet Taste Receptor and Low-Molecular-Weight Sweet Compounds. *PLOS ONE*. DOI:10.1371/journal.pone.0035380. (accessed December 15, 2016).
- [2] Kunishima, N.; Shimada, Y.; Tsuji, Y.; Sato, T.; Yamamoto, M.; Kumasaka, Y.; Nakanishi, S.; Jingami, H.; Morikawa, K. Structural Basis of Glutamate Recognition by a Dimeric Metabotropic Glutamate Receptor. *Nature*. **2000**, *407*, 971–977.
- [3] Maillet, E. L.; Cui, M.; Jiang, P.; Mezei, M.; Hecht, E.; Quijada, J.; Margolskee, R. F.; Osman, R.; Max, M. Characterization of the Binding Site of Aspartame in the Human Sweet Taste Receptor. *Chemical Senses*. **2015**, *40*, 577-586.
- [4] Ouroboros. เรื่องราวของลิ้นและรส (Tongue and taste receptors involvement) [Online]. <http://www.vcharkarn.com/varticle/41515> (accessed February 1, 2017)
- [5] รศ.ดร.สมปอง สรววมศิริ. เอกสารประกอบการเรียน บทที่ 12 Sensory1 [Online]. www.as.mju.ac.th/E-Book/t_sompong/...310/บทที่%2012%20sensory1.docx (accessed February 1, 2017).
- [6] Chandrashekar, J.; Hoon, M. A.; Ryba, N. J.; Zuker, C. S. The Receptors and Cells for Mammalian Taste. *Nature*. **2006**, *444*, 288–294.
- [7] Bachmanov, A. A.; Beauchamp, G. K. Taste Receptor Genes. *Annual Review of Nutrition*. **2007**, *27*, 389–414.
- [8] Li, X.; Staszewski, L.; Xu, H.; Durick, K.; Zoller, M.; Adler, E. Human Receptors for Sweet and Umami Taste. *PNAS*. **2002**, *99*, 4692–4696.
- [9] Pin, J. P.; Galvez, T.; Prezeau, L. Evolution, Structure, and Activation Mechanism of Family 3/C G-Protein-Coupled Receptors. *Pharmacol Ther*. **2003**, *98*, 325–354.
- [10] Scientific Psychic. Sugar Substitutes and Artificial Sweeteners Chemical Structure [Online]. <http://www.scientificpsychic.com/fitness/artificial-sweeteners.html> (accessed December 15, 2016).

- [11] Cheng, J.; Li, J.; Wang, Z.; Eickholt, J.; Deng, X. The MULTICOM Toolbox for Protein Structure Prediction. *BMC Bioinformatics*. **2012**, *13*, 65-76.
- [12] Yousif, R. H.; Khairudin, N. A. Homology Modeling of Human Sweet Taste Receptors: T1R2-T1R3. *Journal of Medical and Bioengineering*. **2014**, *3*, 84-86.
- [13] Chothia, C.; Lesk, A. M. The Relation between the Divergence of Sequence and Structure in Proteins. *EMBO J*. **1986**, *5*, 823-826.
- [14] Jorgensen, W. L. Rusting of the Lock and Key Model for Protein-Ligand Binding". *Science*. **1991**, *254*, 954-955.
- [15] Gagnon, J. K.; Law, S. M.; Brooks, C. L. Flexible CDOCKER: Development and Application of a Pseudo-Explicit Structure-Based Docking Method within CHARMM. *J Comput Chem*. **2016**, *37*, 753-762.
- [16] Murcko, M. A. Computational Methods to Predict Binding Free Energy in Ligand-Receptor Complexes. *Journal of Medicinal Chemistry*. 1995, *38*, 4953-4967.
- [17] Meller, J. Molecular Dynamics. eLS [Online early access]. DOI:10.1002/9780470015902.a0003048.pub2. Published Online: March 2010. <http://www.els.net> (accessed December 20, 2016).
- [18] Case, D. A.; Babin, V.; Berryman, J. T.; Betz, R. M.; Cai, Q.; Cerutti, D. S.; Cheatham, T. E.; Darden, T. A.; Duke, R. E.; Gohlke, H.; Goetz, A. W.; Gusarov, S.; Homeyer, N.; Janowski, P.; Kaus, J.; Kolossváry, I.; Kovalenko, A.; Lee, T. S.; LeGrand, S.; Luchko, T.; Luo, R.; Madej, B.; Merz, K. M.; Paesani, F.; Roe, D. R.; Roitberg, A.; Sagui, C.; Salomon-Ferrer, R.; Seabra, G.; Simmerling, C. L.; Smith, W.; Swails, J.; Walker, R. C.; Wang, J.; Wolf, R. M.; Wu, X.; Kollman, P. A. (2014), AMBER 14, University of California, San Francisco.
- [19] Salomon-Ferrer, R.; Case, D. A.; Walker, R. C. An Overview of the Amber Biomolecular Simulation Package. *WIREs Comput Mol. Sci*. **2013**, *3*, 198-210.

Curriculum Vitae

Miss. Aunchan Opasmahakul was born on June 23, 1995 in Bangkok, Thailand. In 2012, she graduated from the Mathematics-Science program from Sainampeung School, Bangkok, Thailand. In 2013, she was admitted to a Bachelor's degree program: major in Chemistry, Faculty of Science, and minor in Faculty of Communication Arts, Chulalongkorn University and would complete the program in 2017. Her address is 244/375, Thian Suan Village, Ramintra 5 Lane, Ramintra Road, Anusawaree Sub-district, Bangkhen District, Bangkok 10220.

